FDG-PET for prediction of tumour aggressiveness and response to intra-arterial chemotherapy and radiotherapy in head and neck cancer

Yoshimasa Kitagawa[1], Kazuo Sano[1], Sadahiko Nishizawa[2], Mikiko Nakamura[1], Toshiyuki Ogasawara[1], Norihiro Sadato[2], Yoshiharu Yonekura[2]

[1] Department of Dentistry and Oral Surgery, Fukui Medical University, Matsuoka, Fukui 910-1193, Japan
[2] Biomedical Imaging Research Center, Fukui Medical University, Fukui, Japan

Received: 7 May 2002 / Accepted: 26 July 2002 / Published online: 26 October 2002

Abstract. The aim of this study was to evaluate the possible usefulness of fluorine-18 fluorodeoxyglucose positron emission tomography (FDG-PET) for predicting tumour aggressiveness and response to intra-arterial chemotherapy (THP-ADM + 5-FU + carboplatin) and radiotherapy in head and neck carcinomas. Twenty patients with squamous cell carcinoma (SCC) of the head and neck were included in the study. All patients completed the treatment regimen, and each patient underwent two FDG-PET studies, one prior to and one at 4 weeks after the chemoradiotherapy. For the quantitative evaluation of regional FDG uptake in the tumour, standardised uptake values (SUVs) with an uptake period of 50 min were used. The pre-treatment SUV (pre-SUV) and post-treatment SUV (post-SUV) were compared with immunohistologically evaluated tumour proliferative potential (MIB-1 and PCNA), tumour cellularity and other parameters including histological grade, tumour size and stage, clinical response and histological evaluation after therapy. All neoplastic lesions showed high SUVs (mean, 9.75 mg/ml) prior to the treatment, which decreased significantly after the therapy (3.41 mg/ml, $P<0.01$). Pre-SUV did not show any correlation with MIB-1, PCNA, cellularity or other parameters. However, lower post-SUV was significantly correlated with good histological results after therapy (no viable tumour cells, $n=16$). In comparison with moderately differentiated SCCs, well-differentiated SCCs exhibited significantly lower post-SUV and a larger difference between pre- and post-SUVs. Lesions with a high pre-SUV (>7 mg/ml) showed residual tumour cells after treatment in 4 out of 15 patients, whereas patients whose lesions showed a low pre-SUV (<7 mg/ml, five patients) were successfully treated. Four out of six tumours with a post-SUV higher than 4 mg/ml had viable tumour cells, whereas all tumours (14/14) with a post-SUV lower than 4 mg/ml showed no viable tumour cells. Computational multivariate analysis using multiple regression revealed four factors (MIB-1 labelling index, cellularity, the number of MIB-1 labelled tumour cells and tumour size grade) contributing to pre-SUV and pre-post SUV (difference between pre-treatment SUV and post-treatment SUV in each patient) with statistical significance. FDG uptake in the tumour might reflect tumour aggressiveness, which is closely related to the proliferative activity and cellularity. Pre-treatment FDG-PET is useful in predicting the response to treatment, and post-treatment FDG-PET is of value in predicting residual viable tumours. FDG-PET has a profound impact on the treatment strategy for head and neck carcinomas.

Keywords: FDG-PET – Head and neck – Proliferation – MIB-1 – PCNA

Eur J Nucl Med (2003) 30:63–71
DOI 10.1007/s00259-002-0978-z

Yoshimasa Kitagawa (✉)
Department of Dentistry and Oral Surgery,
Fukui Medical University, Matsuoka, Fukui 910-1193, Japan
e-mail: ykitagaw@fmsrsa.fukui-med.ac.jp
Tel.: +81-776-613111, Fax: +81-776-618128

Introduction

Squamous cell carcinoma (SCC) of the head and neck is a histologically distinct but clinically heterogeneous entity including multiple anatomical sites of origin with different natural history and clinical behaviour. Due to these characteristics, it is difficult to accurately predict the efficacy of treatments and the prognosis of patients using conventional clinicopathological criteria. Increasing biological knowledge of head and neck cancer in terms of parameters such as tumour aggressiveness or proliferative activity would help to determine optimal management and evaluate prognosis.

Malignant tumours are characterised by increased glucose metabolism [1], which can be monitored with positron emission tomography (PET) using a glucose analogue, fluorine-18 labelled fluorodeoxyglucose (FDG) [2]. FDG-PET has an advantage over other imaging modalities in detecting change in glucose metabolism, which is closely related to the viability of the cancer cells. FDG-PET has gained acceptance in clinical oncology for the detection and staging of various kinds of malignancies [3, 4]. We have previously shown the clinical value of FDG-PET in head and neck SCCs, for monitoring response to neoadjuvant intra-arterial chemotherapy with concomitant radiotherapy [5].

In vitro assessment of proliferative rates of tumours has advanced with the development of immunohistochemical techniques [proliferation markers such as Ki-67 and proliferating cell nuclear antigen (PCNA)] and DNA flow cytometry, which label cells in different states of biological activity. In certain tumour cell types, glucose metabolism measured by FDG-PET varies proportionally with the proliferative activity and the grade of malignant cells [6, 7, 8]. A few reports have correlated FDG uptake with proliferation in head and neck carcinomas [9, 10, 11]. However, to our knowledge, no previous report has correlated metabolic activity with proliferative activity in relation to response to therapy and prognosis of head and neck cancer.

This study aimed to evaluate the possible usefulness of FDG-PET in predicting tumour aggressiveness and response to intra-arterial chemotherapy and radiotherapy in head and neck carcinomas. For this purpose, we compared regional uptake of FDG with immunohistologically evaluated tumour proliferative potential, tumour cellularity and other clinicopathological parameters.

Materials and methods

Patients. The study was prospectively conducted in 20 consecutive patients with head and neck cancer who completed the treatment regimen described below and underwent two FDG-PET studies, one prior to and one after treatment (17 males and 3 females; mean age, 62.3 years; range, 47–78 years) (Table 1). Biopsy was performed before treatment in all patients for the histopathological and immunohistological evaluation. Biopsy or surgical specimens after treatment were also available for the evaluation of therapeutic effects in all patients. Patients were followed up for 1–7 years (mean, 4 years and 4 months). Patients with previous treatment for cancer, distant metastasis or known diabetes mellitus were excluded from the study. The clinical staging was based on the criteria of the International Union Against Cancer [12] and the American Joint Committee on Cancer TNM classification [13]. The FDG-PET study was performed before biopsy in all patients in order to eliminate the influence of biopsy on the PET results. Twelve of the 20 patients were in stage III or IV. Sixteen patients had a well-differentiated SCC and the remaining four patients had a moderately differentiated one. The study protocol was approved by the Ethical Committee of Fukui Medical University and each patient gave their written informed consent.

Treatment regimen. All 20 patients received neoadjuvant chemoradiotherapy as an organ preservation protocol [5], consisting of two courses of intra-arterial chemotherapy [THP-ADM, 5-FU and carboplatin (CBDCA)] and concomitant radiotherapy (30–40 Gy). In seven patients with a tumour crossing the midline, the arterial catheter was placed bilaterally.

Four weeks after completion of the chemoradiotherapy, the clinical response was evaluated using the WHO criteria [14]. Effects of the therapy were also evaluated histologically using the surgical or biopsy specimens in all patients according to the classification of Shimosato et al. [15].

FDG-PET imaging. All PET imaging procedures used in this study were exactly the same as those used in our previous study [5]. FDG was produced with an automated FDG synthesis system (NKK, Tokyo, Japan) with a small cyclotron (OSCAR3, Oxford Instruments, UK) [16]. PET scanning was performed on a GE Advance scanner (GE, Milwaukee, Wis., USA) [17]. Transmission scan was performed for 10 min using a standard rod source of $^{68}Ge/^{68}Ga$ for attenuation correction of the emission images.

The 20 patients underwent FDG-PET prior to and more than 4 weeks after chemoradiotherapy (mean, 38 days after the treatment). The subjects were administered 244–488 MBq (6.6–13.2 mCi) FDG in a fasting state, delivered via the cubital vein over 10 s. Emission scan was performed for 20 min, starting at 40 min after the injection. The plasma glucose levels were measured in all patients.

Data analysis of PET results. For the quantitative evaluation of FDG uptake in the tumour, regions of interest (ROIs: round in shape and 5 mm in diameter) were placed on the area of highest FDG uptake on the static images. The FDG uptake values were corrected for the injected dose and patient body weight in order to obtain the standardised uptake values (SUVs) as follows:

$$\mathrm{SUV} = \frac{\text{tissue radioactivity concentration (Bq/ml)}}{\text{injected dose (Bq)/body weight (g)}}$$

Finally, we compared the pre-treatment SUV (pre-SUV) and post-treatment SUV (post-SUV) with histological and immunohistochemical results.

Immunohistochemistry for MIB-1 and PCNA. All pre-treatment biopsy specimens were used for MIB-1 (Ki-67) [18] and PCNA staining by the immunoperoxidase (ABC) method.

Paraffin sections of 10% buffered formalin-fixed samples were rehydrated through a graded series of ethanol after deparaffinisation in xylene and then washed in distilled water. For MIB-1, for retrieval of antigenicity, the sections were placed in 0.01 *M* citrate buffer (pH 6.0) and treated three times for 5 min (1 min interval for each irradiation) in a household microwave oven (Toshiba ER-VS2, Tokyo, Japan) at 500 W [19]. The sections were allowed to cool at room temperature (RT) for 20 min. In both MIB-1 and PCNA procedures, endogenous peroxidase activity was blocked by methanol containing 0.3% H_2O_2 for 30 min. Immunostaining was performed using a Vectastain Elite ABC Mouse IgG Kit (Vector Lab., Burlingame, Calif., USA). After rinsing with phosphate-buffered saline (PBS, pH 7.2), non-specific binding was blocked with diluted normal horse serum. The sections were then incubated for 1 h at RT with the primary MIB-1 antibody (Immunotech, Marseille, France; 1:100 diluted with PBS) or primary PCNA antibody (Novocastra Lab., Newcastle, UK; 1:100 diluted with PBS). Sections were then rinsed with PBS and incubated with biotinylated horse anti-mouse IgG for 30 min. After washing with PBS, the

antibody binding sites were demonstrated using 3,3'-diaminobenzidine tetrahydrochloride (DAB; Dojin, Kumamoto, Japan). The sections were lightly counterstained with haematoxylin, dehydrated with ethanol, cleared with xylene and mounted with Entellan Neu (Merck, Darmstadt, Germany). Negative control sections were prepared by performing immunohistochemistry using non-immune mouse isotype IgG1 (DAKO, Glostrup, Denmark; 1:100 diluted with PBS) instead of the primary MIB-1 antibody, and non-immune mouse isotype IgG2a (DAKO, Glostrup, Denmark; 1:100 diluted with PBS) instead of the primary PCNA antibody, respectively.

Quantitative analysis of immunostaining results. Areas with a representative histological pattern of the lesion were randomly observed. Two observers independently evaluated and interpreted the results of immunostaining without knowledge of any clinical information or PET data. At least 1,000 labelled and unlabelled tumour cells were counted with a squared eyepiece graticule (Nikon, Tokyo, Japan) at a magnification of ×400 under an optical microscope (Biophot, Nikon, Tokyo, Japan). Counting was performed within a grid of the eyepiece graticule in a minimum of three fields. The labelling index (LI; %) for MIB-1 or PCNA was calculated as (labelled cells/total cells counted) ×100. The results of the labelling indices in this study were shown as an average of the observation data by the two examiners.

Cellular density (cellularity). Tumour cells were counted by the same examiners in the same high-power fields (magnification ×400) within a grid of the eyepiece graticule in a minimum of three fields to determine cellular density. Cellular density was defined as the number of tumour cells within a grid of the eyepiece graticule at a magnification of ×400 [tumour cells/250 μm× 250 μm (0.0625 mm^2)].

Statistical analysis. The data presented in this paper are expressed as mean±SD. Regression analysis was used to determine the existence of relationships between SUV and labelling indices of MIB-1 and PCNA, cellularity, number of MIB-1 labelled (positive) tumour cells (multiplication of MIB-1 LI by cellularity) and number of PCNA-labelled (positive) tumour cells (multiplication of PCNA LI by cellularity). Analyses for post-SUV and pre-post SUV (difference between pre-treatment SUV and post-treatment SUV in each patient) were also performed in the same manner.

Mann-Whitney *U* test and Kruskal-Wallis test were used to determine differences between pre-SUV, post-SUV and pre-post SUV and histopathological grade (differentiation), tumour category, stage, clinical response and histological evaluation after therapy according to the classification of Shimosato et al. [15].

Multivariate analysis was performed by multiple regression analysis. Probability values of less than 0.05 indicated a statistically significant difference (two tails). All statistical analyses were performed using StatView 5.0 for Macintosh (BNN, Tokyo, Japan).

Results

Table 1 summarises tumour characteristics, response to therapy, FDG uptake values, and histopathological data of each patient.

Response to therapy

Based on the WHO criteria, 15 out of the 20 patients showed a clinically complete response and the remaining five patients were designated as partial responders. Histological evaluation after therapy showed no viable tumour cells (grade 4) in 16 out of 20 patients (80.0%). The remaining four patients had residual tumour cells (grade 0, n=1; grade 2b, n=3).

All pre-treatment FDG-PET studies demonstrated focal FDG uptake corresponding to the known tumour confirmed by biopsy and other imaging modalities or visual inspection. After therapy, all primary lesions showed an obvious decrease in FDG uptake. The mean SUV decreased significantly from 9.75±4.85 mg/ml (range 4.07–26.10 mg/ml) to 3.41±1.58 mg/ml (range 1.12–8.32 mg/ml) (P<0.01). Tumours with residual viable cells (grades 0 and 2b, n=4) showed a post-SUV of 5.54±1.88 mg/ml (range 4.39–8.32). On the other hand, grade 4 tumours without residual tumour cells (n=16) had a significantly lower SUV (P<0.01) of 2.88± 0.98 mg/ml (range 1.12–4.61). Four out of six tumours with post-SUVs higher than 4 mg/ml had viable tumour cells, and showed pre-SUVs higher than 7 mg/ml. On the other hand, all tumours with post-SUVs lower than 4 mg/ml (14/14) were free of viable cells regardless of their pre-SUVs. Lesions with high pre-SUV (>7 mg/ml) showed residual viable tumour cells after the treatment in 4 out of 15 patients, whereas those with low pre-SUVs (<7 mg/ml, five patients) were successfully treated.

With concomitant chemoradiotherapy monitored by FDG-PET, six patients avoided surgery, and the remaining 14 patients underwent a reduced form of surgery. No local recurrence was observed at a maximum follow-up of 7 years (mean, 4 years and 4 months; range, 1 year–7 years). Two patients died of distant metastases (survival period 1 year, and 6 years, respectively) and one died of pneumonia. The remaining 17 patients (85%) now survive free of cancer. The 5-year survival rate was 90%.

Immunohistochemistry for MIB-1 and PCNA, and cellularity

Mean labelling indices for MIB-1 and PCNA were 27.3%±12.1% (range 6.2%–51.8%) and 31.6%±10.5% (range 11.8%–56.6%), respectively. Mean cellularity was 327.2±95.8 (range 203.1–522.1).

Association between SUVs and various parameters

Intense immunoreactivity to MIB-1 or PCNA antigen was present in head and neck carcinomas with low FDG uptake as well as in those with high FDG uptake. No significant correlation was found between pre-SUV and MIB-1 LI or between pre-SUV and PCNA LI (Fig. 1).

Table 1. Patient characteristics, FDG-PET findings and results in respect of immunoreactivity (MIB-1 and PCNA) and cellularity

Patient no.	Age (yrs)	Sex	Location	Differentiation	TNM classification	Stage	Clinical response	Histological evaluation[a]	Pre-SUV	Post-SUV	Pre-post SUV	MIB-1 LI	PCNA LI	Cellularity
1	63	F	Tongue	Well	T 4 N 2b M 0	IV	PR	2b	7.85	4.41	3.44	51.8	41.9	461.3
2	71	M	Tongue	Well	T 2 N 0 M 0	II	CR	4	10.56	3.16	7.40	33.4	26.0	203.1
3	50	M	Tongue	Well	T 4 N 1 M 0	IV	CR	2b	14.12	4.39	9.73	26.4	33.0	386.3
4	66	M	Buccal mucosa	Well	T 3 N 2b M 0	IV	CR	4	5.07	4.25	0.82	26.5	24.2	265.9
5	70	M	Maxillary gingiva	Well	T 2 N 0 M 0	II	CR	4	7.96	2.76	5.19	9.2	35.1	328.9
6	71	F	Tongue	Well	T 2 N 0 M 0	II	CR	4	4.07	1.81	2.26	36.3	27.0	368.5
7	47	M	Lower lip	Well	T 2 N 1 M 0	III	CR	4	11.22	1.12	10.10	16.2	31.3	456.3
8	51	M	Mandible	Moderate	T 4 N 1 M 0	IV	PR	2b	7.28	5.02	2.26	6.2	23.8	273.4
9	66	M	Tongue	Well	T 2 N 0 M 0	II	CR	4	5.15	2.87	2.28	22.9	25.1	210.5
10	48	M	Mandibular gingiva	Well	T 2 N 1 M 0	III	CR	4	7.70	3.52	4.18	31.1	16.5	300.2
11	74	M	Floor of the mouth	Well	T 3 N 1 M 0	III	CR	4	14.54	2.80	11.74	10.0	39.7	346.1
12	60	M	Mandibular gingiva	Well	T 4 N 2a M 0	IV	PR	4	12.77	3.11	9.66	24.2	30.2	302.8
13	68	M	Palatal mucosa	Moderate	T 1 N 0 M 0	I	CR	4	9.76	3.80	5.96	44.9	56.6	315.2
14	63	M	Buccal mucosa	Well	T 3 N 0 M 0	III	CR	4	5.59	2.80	2.79	20.4	33.8	259.1
15	51	F	Tongue	Moderate	T 2 N 0 M 0	II	PR	0	8.54	8.32	0.22	16.8	27.7	302.9
16	64	M	Mandibular gingiva	Well	T 4 N 0 M 0	IV	CR	4	8.40	3.53	4.87	26.4	30.6	240.8
17	71	M	Floor of the mouth	Moderate	T 2 N 0 M 0	II	CR	4	6.60	4.61	1.98	37.9	47.6	503.1
18	58	M	Mandibular gingiva	Well	T 4 N 0 M 0	IV	PR	4	11.34	2.76	8.58	30.4	43.4	522.1
19	56	M	Floor of the mouth	Well	T 4 N 0 M 0	IV	CR	4	26.10	1.61	24.49	37.0	27.1	287.2
20	78	M	Floor of the mouth	Well	T 2 N 0 M 0	II	CR	4	10.46	1.56	8.90	38.9	11.8	209.6
Mean ±SD									9.75 ±4.85	3.41 ±1.58	6.34 ±5.50	27.3 ±12.1	31.6 ±10.5	327.2 ±95.8

Well, Well-differentiated squamous cell carcinoma; Moderate, Moderately differentiated squamous cell carcinoma; CR, complete response; PR, partial response; LI, labelling index (%)

[a] Histological evaluation after therapy according to Shimosato et al. [15]: grade 0, no recognised changes in tumour; grade 2b, tumour destruction is extensive, but viable cell nests are present in small areas of the tumour; grade 4, no tumour cells remaining in any section

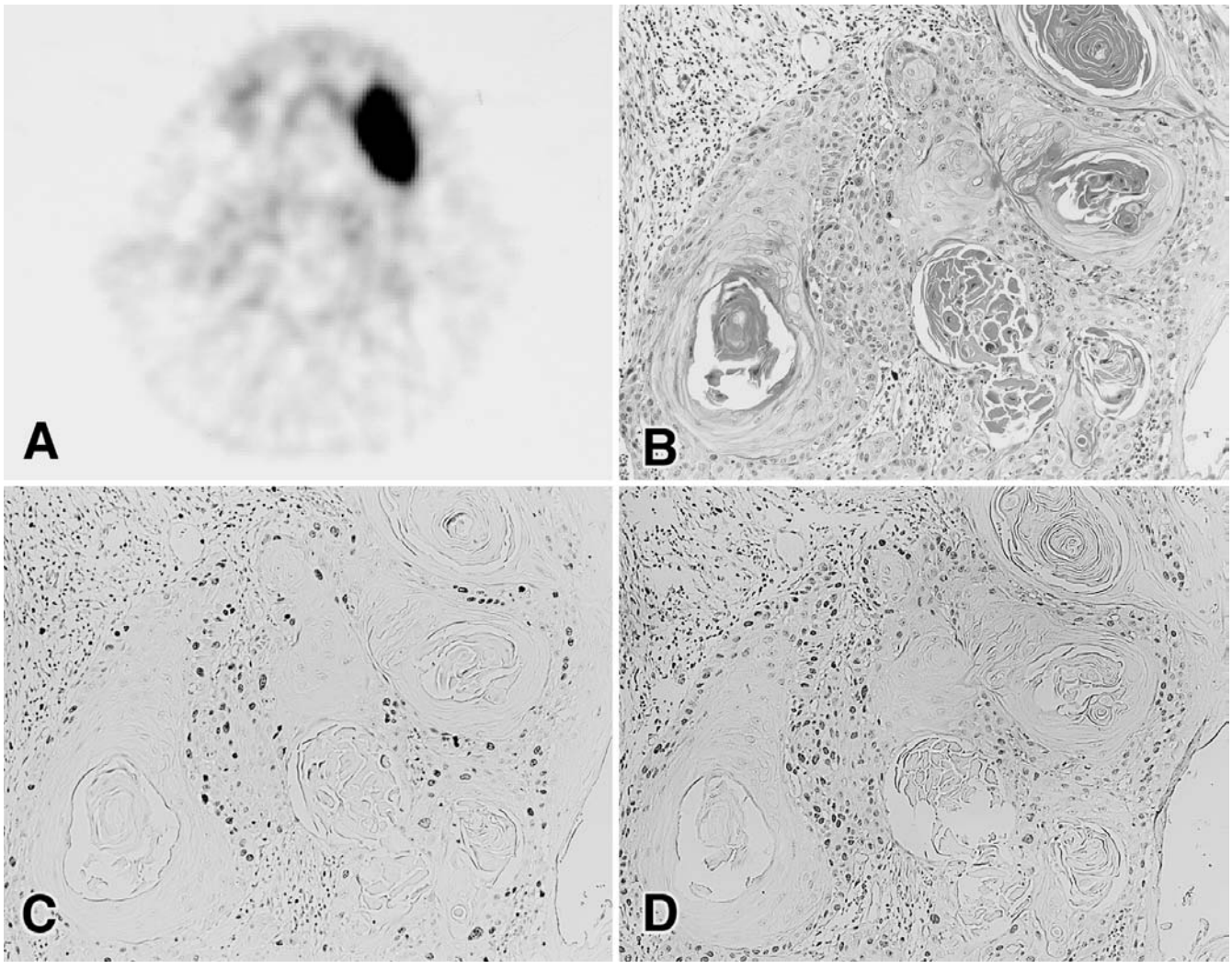

Fig. 1A–D. FDG-PET image and histological and immunohistochemical findings in a 64-year-old male with mandibular gingival cancer. **A** The pre-treatment FDG-PET image shows intense focal accumulation (SUV=8.40 mg/ml) in the tumour. **B** Haematoxylin and eosin staining reveals a well-differentiated squamous cell carcinoma (cellularity =240.8) (magnification ×33). **C, D** Immunohistochemical staining demonstrates MIB-1 positive cells (**C**; MIB-1 labelling index: 26.4%) and PCNA-positive cells (**D**; PCNA labelling index: 30.6%) in the nuclei of peripheral cells of the tumour nest (magnification ×33)

Regression analysis also revealed no significant correlation between pre-SUV and cellularity.

Statistical analysis showed no significant difference in pre-SUV between subgroups of each parameter (histological grade, tumour size, stage and so on). However, Mann-Whitney *U* test showed statistically significant differences in post-SUV between histological grades (differentiation). In addition, with regard to the difference between pre-SUV and post-SUV (pre-SUV minus post-SUV: pre-post SUV), a higher pre-post SUV was associated with greater tumour differentiation (Table 2).

Multivariate analysis

Eight factors (histological grade, tumour size, stage, MIB-1 LI, PCNA LI, cellularity, MIB-1 labelled tumour cells, and PCNA labelled tumour cells) were evaluated by the multivariate analysis for SUV. The analysis revealed the multiple regression equations with statistical significance as follows:

$$\begin{aligned}\text{Pre}-\text{SUV} = &-33.558+1.188\times(\text{MIB}-1\text{LI})\\ &+0.1\times(\text{cellularity})-0.328\\ &\times(\text{number of MIB}-1\text{ labelled tumour cells})\\ &+2.948\times(\text{tumour size grade})\end{aligned}$$

F value=3.690 (P=0.0277), R^2=0.496 (R=0.704). The above four regression coefficients were statistically significant (MIB-1 LI: P=0.0055; cellularity: P=0.0092; MIB-1 labelled tumour cells: P=0.0062; tumour size grade: P=0.0077).

$$\begin{aligned}\text{Pre}-\text{postSUV} = &-48.577+1.555\times(\text{MIB}-1\text{LI})\\ &+0.13\times(\text{cellularity})-0.429\\ &\times(\text{number of MIB}\\ &-1\text{ labelled tumour cells})\\ &+3.235\times(\text{tumour size grade})\end{aligned}$$

Table 2. Relationship between SUVs and various parameters

Parameter	Class	Pre-SUV		Post-SUV		Pre-post SUV	
		Mean (range)	*P* value	Mean (range)	*P* value	Mean (range)	*P* value
Histological grade			0.4497		0.0061*		0.0421*
(differentiation)	Well (*n*=16)	10.18 (4.07–26.10)		2.90 (1.12–4.41)		7.28 (0.82–24.49)	
	Moderate (*n*=4)	8.04 (6.60–9.76)		5.44 (3.80–8.32)		2.61 (0.22–5.96)	
Primary tumour size			0.2309		0.7276		0.4475
	T1+T2 (*n*=10)	8.20 (4.07–11.22)		3.35 (1.12–8.32)		4.85 (0.22–10.10)	
	T3 (*n*=3)	8.40 (5.07–14.54)		3.28 (2.80–4.25)		5.12 (0.82–11.74)	
	T4 (*n*=7)	12.55 (7.28–26.10)		3.55 (1.61–5.02)		9.00 (2.26–24.49)	
UICC stage			0.2170		0.9692		0.1533
	I+II (*n*=8)	7.89 (4.07–10.56)		3.61 (1.56–8.32)		4.27 (0.22–8.90)	
	III+IV (*n*=12)	11.00 (5.07–26.10)		3.28 (1.12–5.02)		7.72 (0.82–24.49)	
Clinical response			0.6312		0.0972		0.4319
	CR (*n*=15)	9.82 (4.07–26.10)		2.97 (1.12–4.61)		6.85 (0.82–24.49)	
	PR (*n*=5)	9.56 (7.28–12.77)		4.72 (2.76–8.32)		4.83 (0.22–9.66)	
Histological evaluation			0.9247		0.0046*		0.2770
after therapy	No viable cells (*n*=16)	9.83 (4.07–26.10)		2.88 (1.12–4.61)		6.95 (0.82–24.49)	
	Residual viable cells (*n*=4)	9.45 (7.28–14.12)		5.54 (4.39–8.32)		3.91 (0.22–9.73)	
MIB-1 labelling index (%)			>0.9999		0.7283		0.9078
	≦25 (*n*=8)	9.13 (5.15–14.54)		3.60 (1.12–8.32)		5.53 (0.22–11.74)	
	>25 (*n*=12)	10.17 (4.07–26.10)		3.28 (1.61–4.61)		6.88 (0.82–24.49)	
PCNA labelling index (%)			0.5892		0.5889		0.5890
	≦32 (*n*=12)	9.78 (4.07–26.10)		3.32 (1.12–8.32)		6.45 (0.22–24.49)	
	>32 (*n*=8)	9.72 (5.59–14.54)		3.54 (2.76–4.61)		6.18 (1.98–11.74)	
Cellularity			0.5184		0.6483		0.3618
	≦310 (*n*=11)	9.78 (5.07–26.10)		3.61 (1.56–8.32)		6.17 (0.22–24.49)	
	>310 (*n*=9)	9.72 (4.07–14.54)		3.16 (1.12–4.61)		6.55 (1.98–11.74)	
MIB-1 × cellularity			0.6761		0.8196		0.5432
	≦80 (*n*=11)	8.82 (5.07–14.54)		3.61 (1.12–8.32)		5.21 (0.22–11.74)	
	>80 (*n*=9)	10.89 (4.07–26.10)		3.16 (1.56–4.61)		7.72 (1.98–24.49)	
PCNA × cellularity			0.1649		0.9692		0.1648
	≦100 (*n*=12)	9.31 (4.07–26.10)		3.46 (1.56–8.32)		5.84 (0.22–24.49)	
	>100 (*n*=8)	10.42 (6.60–14.54)		3.33 (1.12–4.61)		7. 09 (1.98–11.74)	

*All statistical tests were performed at the 5% level of significance

F value=5.077 (P=0.0087), R^2=0.575 (R=0.758). The above four regression coefficients were statistically significant (MIB-1 LI: P=0.001; cellularity: P=0.0019; MIB-1 labelled tumour cells: P=0.0012; tumour size grade: P=0.0054).

Multivariate analyses with the other variables showed no statistical significance.

Discussion

FDG uptake is fundamentally a measure of energy metabolism. Therefore, we hypothesised that pathological characteristics, such as high proliferative activity and high tumour cellularity, might be related to elevated SUV in untreated head and neck cancer. However, no single factor explained elevated FDG uptake by itself.

Data on FDG uptake in association with proliferative activity or with cellularity in malignant tumours are controversial. Okada et al. compared FDG uptake and cellular proliferation in 23 patients with malignant lymphomas of the head and neck, and found that tumour proliferative activity assessed by Ki-67 immunoreactivity increased in proportion to increases in FDG uptake [8]. In addition, FDG accumulation has been shown to correlate with the proliferative index measured by DNA flow cytometry in head and neck tumours [9, 10, 11, 20]. The presence of a similar relationship has been reported in other malignant tumours [21, 22, 23, 24].

In contrast, Buck et al. recently found no correlation between proliferative activity and FDG uptake in pancreatic cancer [25]. Higashi et al., in an in vitro study, showed that FDG accumulation has a close relationship with the number of viable tumour cells rather than with proliferative activity [26]. In clinical studies, cellularity, rather than proliferative activity, has been suggested to have a significant relationship to FDG uptake in rectal cancer [27], pancreatic cancer [28, 29] and other tumours [30, 31].

In our study, the multivariate analysis revealed four factors (MIB-1 LI, cellularity, the number of MIB-1 labelled tumour cells and tumour size grade) contributing to high pre-SUV and pre-post SUV with statistical significance. These findings suggest that under the conditions of higher tumour cellularity, increased expression of MIB-1 immunoreactivity and larger tumour size, head and neck carcinomas have higher FDG uptake in the tumour cell. Furthermore, under the same conditions, tumours could be expected to show good sensitivity to our chemoradiotherapy regimen. In other words, FDG accumulation and the efficacy of chemoradiotherapy are closely related to cellularity, MIB-1 LI and tumour size, which are supposed to express biological tumour characteristics, including aggressiveness, in head and neck cancers. The results obtained seemed to support our hypothesis.

This study showed advantages of FDG-PET over conventional criteria in monitoring patients throughout treatment. Compared with moderately differentiated tumours, well-differentiated SCCs responded better to our chemoradiotherapy, showing significantly lower post-SUV, a larger absolute reduction in tumour size and a larger difference between pre- and post-SUV. These characteristics are useful for predicting response to therapy. Beside the differentiation of tumours, pre-SUV itself was useful in predicting the response to therapy. Tumours with a high pre-SUV (>7 mg/ml) appeared to be more resistant to treatment than those with a low pre-SUV. This may be because higher FDG uptake indicates greater cell viability or a higher propensity for cells to divide, or both [10, 26].

Post-SUV was also useful for predicting the presence or absence of residual tumour cells. In this study, the quantitative threshold value for differentiating the presence or absence of residual tumour cells was tentatively determined as a post-SUV of 4.0 mg/ml. With this cut-off value, all four lesions with viable tumour cells after treatment could be diagnosed as true-positive (sensitivity, 100%), and all tumours with post-SUVs lower than 4 mg/ml (14/14) were free of viable tumour cells regardless of their pre-SUVs. Therefore, by providing a precise assessment of the efficacy of chemoradiotherapy prior to surgery, post-SUV is of great significance in enabling a decision to be made regarding the optimal surgical option in each patient. This information would never be available by means of immunohistochemical and morphological evaluations.

We have already attempted to determine the selection of further treatment based on the FDG-PET data. In six patients, who showed a post-SUV lower than 4.0 mg/ml in addition to complete response, surgery was avoided. In these patients, no recurrence was observed at a mean follow-up of more than 4 years. The remaining 14 patients underwent reduced conservative surgery, with resultant clinical advantages in terms of lower risk of aesthetic problems and greater preservation of oral function. Follow-up data showed a 5-year survival rate of 90%. These results suggest that FDG-PET is a powerful tool in assessing the therapeutic effect and can contribute to the improvement of the quality of life of patients with head and neck carcinomas.

Limitations of the study

Although the post-SUV was very useful in predicting the presence or absence of residual tumour cells, a false positive result was obtained in two patients. Because of a prolonged inflammatory reaction after radiation therapy, we waited more than 4 weeks after completion of the therapy for the post-treatment evaluation by FDG-PET. Even after more than 4 weeks, however, an inflammatory reaction may continue in some patients, potentially affecting FDG uptake. Actually in these patients, no residual tumour cells were found in the surgical specimen.

Many reports have suggested an association between increased SUV and single factors such as proliferative activity, cellularity and so on [8, 9, 10, 11, 20, 26, 27, 28, 29, 30, 31]. Although our study demonstrated several factors contributing to the pre-treatment SUV, we could not find a single factor that explained the high SUV by itself. This may be partly explained by the fact that head and neck carcinomas are a heterogeneous entity including multiple anatomical sites of origin. The shape and size of the tumour may affect the SUV because of the partial volume effect; this is especially true in the case of thin superficial tumours. Another explanation may be the difference in sampled area between the methods for evaluation. The stained sections for immunohistochemistry and cellularity scoring may not correspond exactly to representative areas of FDG uptake on PET images. Biopsy specimens just provide information on a limited part of the tumour, whereas FDG uptake on PET images, representing energy metabolism, reflects biological activity of the tumour as a whole.

Conclusion

FDG-PET provides a non-invasive functional image reflecting the biological metabolism of the whole tumour, and is of great benefit in terms of clinical cancer management. Cellularity, MIB-1 labelling index and tumour size (i.e. biological tumour aggressiveness) play an essential role both in FDG accumulation and in efficacy of the chemoradiotherapy. Pre-treatment FDG-PET is useful in predicting the response to treatment, and post-treatment FDG-PET is of value in predicting the presence or absence of residual tumour. FDG-PET will have a profound impact on the treatment strategy for head and neck carcinomas.

Acknowledgements. This study was supported in part by Grant-in-Aid for Scientific Research (C, No. 11671982) from the Ministry of Education, Science, Sports and Culture, Japan.

References

1. Flier JS, Mueckler MM, Usher P, Lodish HF. Elevated levels of glucose transport and transporter messenger RNA are induced by *ras* or *src* oncogenes. *Science* 1987; 235:1492–1495.
2. Som P, Atkins HL, Bandoypadhyay D, Fowler JS, MacGregor RR, Matsui K, Oster ZH, Sacker DF, Shiue CY, Turner H, Wan CN, Wolf AP, Zabinski SV. A fluorinated glucose analog, 2-fluoro-2-deoxy-D-glucose (F-18): nontoxic tracer for rapid tumor detection. *J Nucl Med* 1980; 21:670–675.
3. Strauss LG, Conti PS. The applications of PET in clinical oncology. *J Nucl Med* 1991; 32:623–648.
4. Bar-Shalom R, Valdivia AY, Blaufox MD. PET imaging in oncology. *Semin Nucl Med* 2000; 30:150–185.
5. Kitagawa Y, Sadato N, Azuma H, Ogasawara T, Yoshida M, Ishii Y, Yonekura Y. FDG PET to evaluate combined intra-arterial chemotherapy and radiotherapy for head and neck neoplasms. *J Nucl Med* 1999; 40:1132–1137.
6. Di Chiro G, DeLaPaz RL, Brooks RA, Sokoloff L, Kornblith PL, Smith BH, Patronas NJ, Kufta CV, Kessler RM, Johnston GS, Manning RG, Wolf AP. Glucose utilization of cerebral gliomas measured by [^{18}F] fluorodeoxyglucose and positron emission tomography. *Neurology* 1982; 32:1323–1329.
7. Duhaylongsod FG, Lowe VJ, Patz EF Jr, Vaughn AL, Coleman RE, Wolfe WG. Lung tumor growth correlates with glucose metabolism measured by fluoride-18 fluorodeoxyglucose positron emission tomography. *Ann Thorac Surg* 1995; 60:1348–1352.
8. Okada J, Yoshikawa K, Itami M, Imaseki K, Uno K, Itami J, Kuyama J, Mikata A, Arimizu N. Positron emission tomography using fluorine-18-fluorodeoxyglucose in malignant lymphoma: a comparison with proliferative activity. *J Nucl Med* 1992; 33:325–329.
9. Minn H, Joensuu H, Ahonen A, Klemi P. Fluorodeoxyglucose imaging: a method to assess the proliferative activity of human cancer in vivo. Comparison with DNA flow cytometry in head and neck tumors. *Cancer* 1988; 61:1776–1781.
10. Haberkorn U, Strauss LG, Reisser C, et al. Glucose uptake, perfusion and cell proliferation in head and neck tumors: relation of positron emission tomography to flow cytometry. *J Nucl Med* 1991; 32:1548–1555.
11. Jacob R, Welkoborsky HJ, Mann WJ, Jauch M, Amedee R. [Fluorine-18]fluorodeoxyglucose positron emission tomography, DNA ploidy and growth fraction in squamous-cell carcinomas of the head and neck. *ORL J Otorhinolaryngol Relat Spec* 2001; 63:307–313.
12. Hermanek P, Sobin LH, eds. *UICC: TNM classification of malignant tumours, 4th edn.* Berlin Heidelberg New York: Springer, 1987.
13. Beahrs OH, Henson DE, Hutter RVP, Kennedy BJ, eds. *Manual for staging of cancer, 4th edn.* Philadelphia: Lippincott, 1992.
14. World Health Organization. *Handbook for reporting results of cancer treatment*. Geneva: World Health Organization, 1979.
15. Shimosato Y, Oboshi S, Baba K. Histological evaluation of effects of radiotherapy and chemotherapy for carcinomas. *Jpn J Clin Oncol* 1971; 1:19–35.
16. Hamacher K, Coenen HH, Stoecklin G. Efficient stereospecific synthesis of no-carrier-added 2-[^{18}F]-fluoro-2-deoxy-D-glucose using aminopolyether supported nucleophilic substitution. *J Nucl Med* 1986; 27:235–238.
17. DeGrado TR, Turkington TG, Williams JJ, et al. Performance characteristics of a whole-body PET scanner. *J Nucl Med* 1994; 35:1398–1406.
18. Sano K, Yoshida S, Ninomiya H, Ikeda H, Ueno K, Sekine J, Iwamoto H, Uehara M, Inokuchi T. Assessment of growth potential by MIB-1 immunohistochemistry in ameloblastic fibroma and related lesions of the jaws compared with ameloblastic fibrosarcoma. *J Oral Pathol Med* 1998; 27:59–63.
19. Key G, Becker MH, Baron B, Duchrow M, Schluter C, Flad HD, Gerdes J. New Ki-67-equivalent murine monoclonal antibodies (MIB 1–3) generated against bacterially expressed parts of the Ki-67 cDNA containing three 62 base pair repetitive elements encoding for the Ki-67 epitope. *Lab Invest* 1993; 68:629–636.
20. Minn H, Clavo AC, Grenman R, Wahl RL. In vitro comparison of cell proliferation kinetics and uptake of tritiated fluorodeoxyglucose and L-methionine in squamous-cell carcinoma of the head and neck. *J Nucl Med* 1995; 36:252–258.

21. Higashi K, Ueda Y, Yagishita M, Arisaka Y, Sakurai A, Oguchi M, Seki H, Nambu Y, Tonami H, Yamamoto I. FDG PET measurement of the proliferative potential of non-small cell lung cancer. *J Nucl Med* 2000; 41:85–92.
22. Vesselle H, Schmidt RA, Pugsley JM, Li M, Kohlmyer SG, Vallires E, Wood DE. Lung cancer proliferation correlates with [F-18]fluorodeoxyglucose uptake by positron emission tomography. *Clin Cancer Res* 2000; 6:3837–3844.
23. Avril N, Menzel M, Dose J, Schelling M, Weber W, Janicke F, Nathrath W, Schwaiger M. Glucose metabolism of breast cancer assessed by ^{18}F-FDG PET: histologic and immunohistochemical tissue analysis. *J Nucl Med* 2001; 42:9–16.
24. Lippitz B, Cremerius U, Mayfrank L, Bertalanffy H, Raoofi R, Weis J, Bocking A, Bull U, Gilsbach JM. PET-study of intracranial meningiomas: correlation with histopathology, cellularity and proliferation rate. *Acta Neurochir Suppl* 1996;65: 108–111.
25. Buck AC, Schirrmeister HH, Guhlmann CA, Diederichs CG, Shen C, Buchmann I, Kotzerke J, Birk D, Mattfeldt T, Reske SN. Ki-67 immunostaining in pancreatic cancer and chronic active pancreatitis: does in vivo FDG uptake correlate with proliferative activity? *J Nucl Med* 2001; 42:721–725.
26. Higashi K, Clavo AC, Wahl RL. Does FDG uptake measure proliferative activity of human cancer cells? In vitro comparison with DNA flow cytometry and tritiated thymidine uptake. *J Nucl Med* 1993; 34:414–419.
27. Ito K, Kato T, Ohta T, Tadokoro M, Yamada T, Ikeda M, Nishino M, Ishigaki T, Gambhir S. Fluorine-18 fluoro-2-deoxyglucose positron emission tomography in recurrent rectal cancer: relation to tumour size and cellularity. *Eur J Nucl Med* 1996; 23:1372–1377.
28. Kato T, Fukatsu H, Ito K, Tadokoro M, Ota T, Ikeda M, Isomura T, Ito S, Nishino M, Ishigaki T. Fluorodeoxyglucose positron emission tomography in pancreatic cancer: an unsolved problem. *Eur J Nucl Med* 1995; 22:32–39.
29. Higashi T, Tamaki N, Torizuka T, Nakamoto Y, Sakahara H, Kimura T, Honda T, Inokuma T, Katsushima S, Ohshio G, Imamura M, Konishi J. FDG uptake, GLUT-1 glucose transporter and cellularity in human pancreatic tumors. *J Nucl Med* 1998; 39:1727–1735.
30. Herholz K, Pietrzyk U, Voges J, Schroder R, Halber M, Treuer H, Sturm V, Heiss WD. Correlation of glucose consumption and tumor cell density in astrocytomas. A stereotactic PET study. *J Neurosurg* 1993; 79:853–858.
31. Berger KL, Nicholson SA, Dehdashti F, Siegel BA. FDG PET evaluation of mucinous neoplasms: correlation of FDG uptake with histopathologic features. *AJR Am J Roentgenol* 2000; 174:1005–1008.